

Article

High-Precision Roller Supported by Active Magnetic Bearings

Cheol Hoon Park ^{1,*}, Tae Gwang Yoon ², Dongwoo Kang ¹ and Hugo Rodrigue ^{3,*}¹ Department of Robotics & Mechatronics, Korea Institute of Machinery & Materials, Daejeon 34103, Korea; dwkang@kimm.re.kr² Magnetar Inc., Daejeon 34103, Korea; mag1@magnetar.co.kr³ School of Mechanical Engineering, Sungkyunkwan University, Suwon 16419, Korea

* Correspondence: parkch@kimm.re.kr (C.H.P.); rodrigue@skku.edu (H.R.); Tel.: +82-42-868-7980 (C.H.P.); +82-31-299-4860 (H.R.)

Received: 17 September 2019; Accepted: 14 October 2019; Published: 17 October 2019

**Featured Application:** Printing machines, Roller conveyors, Cleanroom applications.

Abstract: Magnetic bearings support rotors in a non-contact way using magnetic force. Therefore, there is no friction and it is possible to measure and control the position of a rotor in the air gap. In this study, the rotational vibration of a roller was minimized using magnetic bearings, and a precision roller capable of automatic alignment using the position control function of magnetic bearings was proposed. A rotation accuracy of approximately 4.6 μm (peak-to-peak) was observed, even under a rotation of 30 rev/min and a radial force load of 300 N. The rotor position control experiment for magnetic bearings showed that 1- μm resolution position control is possible. To further improve the accuracy, the automatic alignment algorithm was proposed using magnetic bearings for the roller misalignment condition, and it was confirmed that alignment is possible at a level that the pressing force difference between both ends of the roller is within 0.3 N. Through this study, it was confirmed that rollers with magnetic bearings can be applied to precision equipment. It is expected that the implementation of the automatic alignment function will simplify the equipment configuration and maintenance compared to conventional rollers with ball bearings.

Keywords: magnetic bearings; automatic alignment; high precision roller; roller applications

1. Introduction

Display devices, such as flexible OLED, micro LED, electronic papers, RFID sensors, solar panels and other electronic elements can be mass-produced in a continuous manner similar to newspapers. Thus, the low-cost mass-production of printed electronics technology is attracting considerable attention [1,2]. In particular, since display devices are composed of fine patterns with features ranging in size from a few μm to tens of μm , the roller must have a vibration amplitude smaller than this feature size. Ideally, the vibration amplitude should remain within a few μm . The vibration of the roller and the application of an ever force during printing are some of the most important factors directly affecting the printing accuracy. Therefore, the roller used for printing requires extremely precise printing surface processing and low rotational vibration. Commonly used printing machines for producing sub-micron patterns include roll-based nanoimprinting and reverse offset printing. In addition, since printing forces significantly affect the patterning mechanism and printing quality [3,4], printing machines for producing sub-micron patterns must have high-precision printing force control and a uniform printing force. For multi-step continuous roll-to-roll printing technology, the tension control of the web [5], the roll of paper used in offset printing, using the roller and longitudinal displacement control are also

important to reduce printing errors [6]. Furthermore, the implementation of proper roller alignment is one of the most important factors in achieving high printing precision and a uniform printing force.

In general, rollers are supported by ball bearings. In the case of printed electronics equipment, the performance improvement and commercialization of printed electronics elements are hindered by the poor rotation accuracy or difficulties during the roller alignment process. Most printing equipment under research/development uses rollers with ball bearings. Ball bearings exhibit significant mechanical wobble, which produces rotational vibrations with at least 10–20 μm of displacement owing to non-uniform stiffness and clearance [7]. In addition, rollers tend to shift during roll-to-roll printing, which causes misalignment of the printing rollers such that disassembly and re-assembly of the printing rollers is required during the production process. Due to this, it is extremely difficult and time-consuming to implement reliable precision printing. A non-uniform force distribution on the printing surface causes periodic errors due to the printing force, and may cause serious printing defects such as nanoimprinting, microcontact printing, and offset printing [8–12]. The printing force applied by rollers must be uniform to improve the printing quality. For this, many additional devices are required, including various force and position sensors, pneumatic or hydraulic actuators, linear motors, and voice coil motors, which make the structure of the printing equipment complicated and more expensive while still requiring periodic re-calibration [13].

Magnetic bearings cause constant bearing stiffness with no friction because they support rollers in a non-contact way, while controlling the magnetic force [14]. This makes the rotational vibration of the roller very small. In addition, since the positions of both ends of the roller can be arbitrarily and easily changed within the air gaps between the shaft core and the electromagnets of the magnetic bearings, it is possible to automatically align the roller so that the printing forces at both ends of the roller can act uniformly. Active magnetic bearings have been used for a wide range of applications including rotors [15], turbo blowers [16], control moment gyroscopes [17], gears [18], and for machining [19]. Existing magnetic bearing rotational machinery focus on the performance of rotating shafts during transmission of a torque, but no study has been done on the use of magnetic bearings to transmit a force as would be required of rollers. Furthermore, the surveyed literature does not include any function for self-aligning rollers that could significantly increase the printing performance for printed electronics.

In this study, a concept for a roller with force feedback for self-alignment making use of magnetic bearings to adjust and align the printing forces without re-assembly was designed and fabricated for precision printing. Its basic performance was tested, and the automatic alignment function was implemented and verified. The measured rotation vibration of this system under a lateral load was measured to be much less than existing rollers with ball bearings. The fine displacement movement performance of the roller using the position control of the magnetic bearings was examined, and the automatic alignment performance was experimentally verified. This study proposes the applicability of a new type of roller to precision printing equipment.

2. Automatic Alignment System Using Magnetic Bearings

For roll-to-roll or roll-to-plate type printing, alignment between the roller and printing surface is required for uniform printing quality. The alignment degree of a roller can be defined as the mechanical parallelism between the roller and printing surface or the uniformity of the printing force at both ends of the roller. For rollers with typical ball bearings, repetitive measurement, disassembly and re-assembly processes are required to adequately align the roller and printing section. In addition, during printing, additional driving devices are required to apply uniform printing forces to both ends of the roller. However, the roller can move freely within the air-gap range and the printing force at each end of the roller can be controlled when magnetic bearings are used as the radial bearings at both ends of the roller. Therefore, the printing forces at both ends of the roller can be controlled to apply a uniform pressure. Furthermore, it is possible to implement the automatic alignment function of the roller by using this characteristic.

2.1. Magnetic Bearing System Configuration

Magnetic bearings can measure and control the position of the rotor using electromagnets, sensors, and control systems. Figure 1 shows the schematic diagram of the magnetic bearing control system. The position of the shaft within the air gap is measured using the gap sensors placed in the x and y directions. The magnetic bearing controller adjusts the position of the shaft core by controlling the input current of the magnetic bearing coil supplied through the current driver. The magnetic bearing controller consists of a proportional-integral-derivative (PID) controller with a sampling frequency of 10 kHz, a lead compensator, and a low-pass filter. The PID gain was optimized to stably levitate the rotor and secure a phase margin of more than 20°.

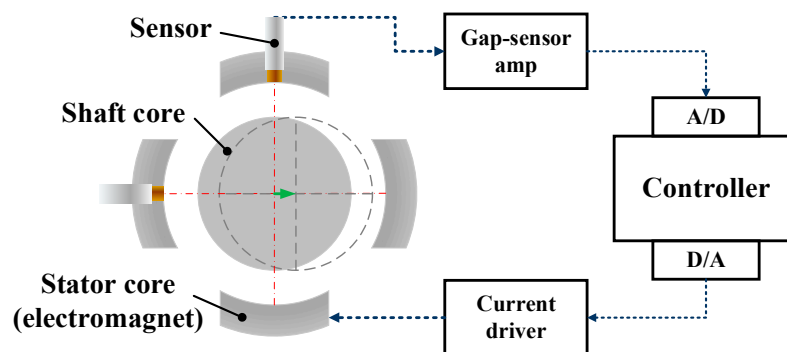


Figure 1. Schematic diagram of magnetic bearing control system.

2.2. Principles of the Automatic Alignment System Using Magnetic Bearings

Figure 2 shows the testing setup for assessing the automatic alignment performance of the precision roller for printing. Radial magnetic bearings capable of controlling the radial position and force were installed at both ends of the roller, and a thrust magnetic bearing was placed at the right end of the roller to control the axial movement. Inside the radial magnetic bearings, gap sensors were attached in the x-axis and y-axis directions to measure the displacement of the rotor in real time. Through the feedback of the gap sensors on the measured roller displacement, the position of the roller inside the air gap was controlled. The roller proposed in this study can move up to ± 0.2 mm in the radial direction from the center of the radial magnetic bearings and the force and position of each of the left and right magnetic bearings can be controlled. The position of the radial bearings can be used to adjust the force exerted by the roller and the load cells provide force feedback of the contact force and alignment of the roller with respect to the element the roller is in contact with. Figure 3 is a conceptual diagram of the automatic alignment of the roller and shows the definition of alignment used in this paper. If the printing forces are the same, it is assumed that alignment is achieved.

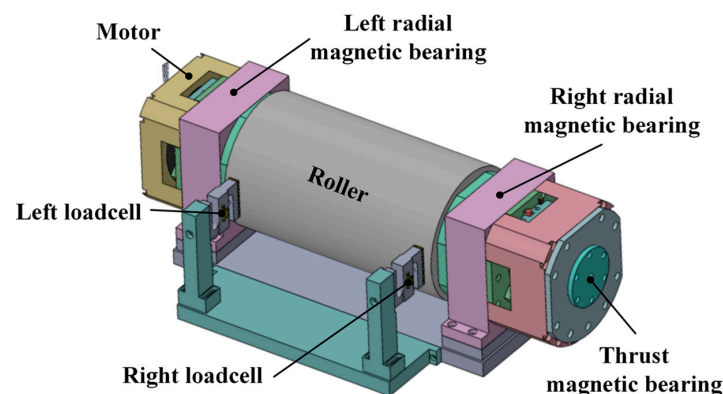


Figure 2. Precision roller testing setup with magnetic bearings for automatic alignment performance assessment.

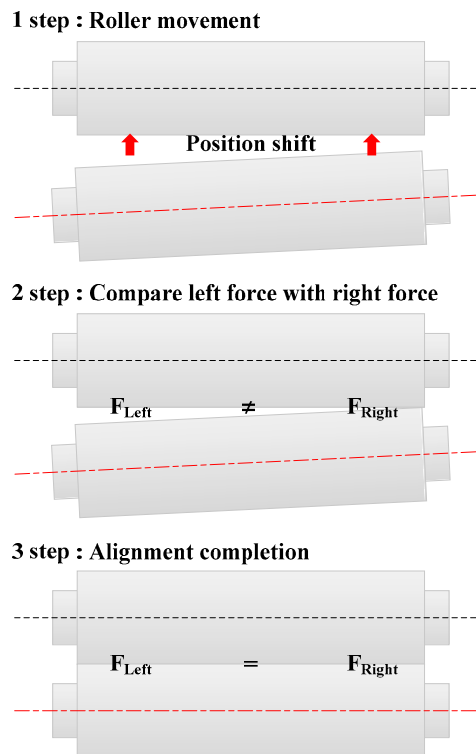


Figure 3. Basic concept of automatic alignment of roller.

3. Design of Magnetic Bearing and Roller System

Figure 4 shows the configuration of the precision roller system with magnetic bearings. The radial magnetic bearings applied to the precision roller for printing must be able to support the printing force as well as the mass of the roller, because the mass of the roller acts as a radial load. The mass of the roller is 30 kg and the maximum printing force applied to the roller during printing was set to 300 N. Therefore, the magnetic bearings must be capable of generating a force of at least 600 N. Based on this, the radial magnetic bearings were designed to generate a force each exceeding 300 N. In the case of the axial force, the thrust generated between the core and rotor magnet in the motor and the axial component of the printing force caused by the vibration and misalignment occurring during the rotation of the roller act as axial disturbances. Since these forces are not large, the required force of the thrust magnetic bearing was set to 100 N. The roller, rotor of the motor, roller printing section, and shaft core were designed to be integrated as one part for ease of control and complete levitation. The design parameters of the radial and axial magnetic bearings were selected based on the magnetic circuit and the magnetic force equation, and they were examined using Maxwell, a finite element electromagnetic field analysis software program [20,21]. The dimensions of the magnetic bearings were selected based on the roller used for the test, but these dimensions may need to be increased depending on the specific application and roller used because larger bearings will be required to support heavier industrial rollers. This process is omitted from this paper for brevity. The air gap of ± 0.2 mm in which the roller can move was designed to implement the automatic alignment function of the roller. This movement range is sufficient for most production processes where the adjustment is fairly small, but the current or the magnetic bearing size might need to be increased to generate the same magnetic force for larger movement ranges. The specifications of the precision roller and magnetic bearings proposed in this study are listed in Table 1.

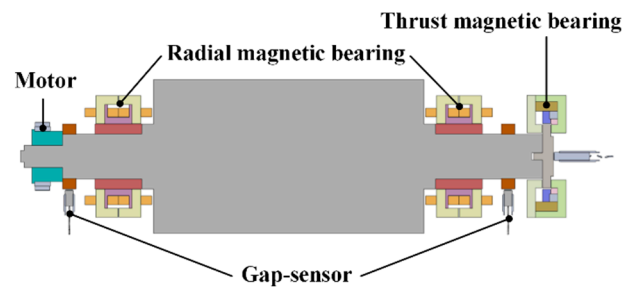


Figure 4. Configuration of precision roller with magnetic bearings for automatic alignment function.

Table 1. Specifications of magnetic bearings.

Item	Value
Radial magnetic bearing outer diameter	72 mm
Radial magnetic bearing required force	300 N
Radial magnetic bearing movement range	± 0.2 mm
Thrust magnetic bearing required force	100 N
Roller diameter	170 mm
Roller length	300 mm
Roller weight	30 kgf
Roller rotation speed	30 rev/min

The prototypes of the magnetic bearings and precision roller equipment for printing were fabricated according to the design parameters shown previously. Figure 5a,b shows the fabricated radial and thrust magnetic bearings, and Figure 5c presents the precision roller. For roller rotation, a direct drive motor (TBMS-12913, Kollmorgen, Radford, VA, United States) was used.

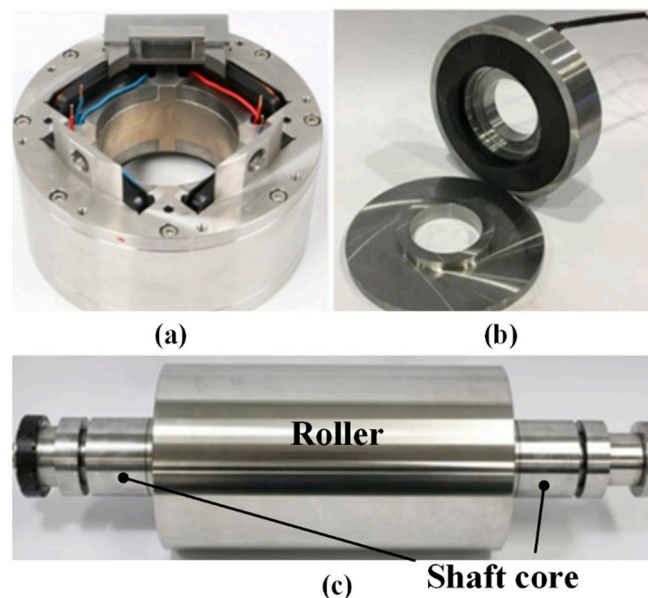


Figure 5. Fabricated roller and magnetic bearings for automatic alignment function: (a) radial magnetic bearing; (b) thrust magnetic bearing; and (c) precision roller.

4. Basic Performance Test of Precision Roller with Magnetic Bearings

The basic performance of the actuator to produce minimal vibration when subjected to a lateral load and to produce step-wise increase in lateral forces was verified. To implement automatic alignment on the rollers, good performance of these two characteristics is essential. Figure 6 shows the conceptual diagram of the roll-to-roll load condition test used to evaluate the basic performance of the actuator,

and Figure 7 illustrates the experimental setup constructed based on the diagram where the idle roller has a diameter of 100 mm.

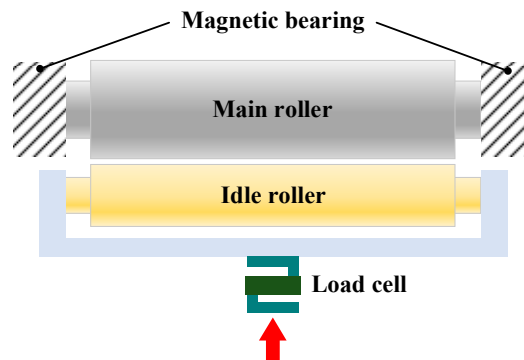


Figure 6. Conceptual diagram of roll-to-roll load condition test.

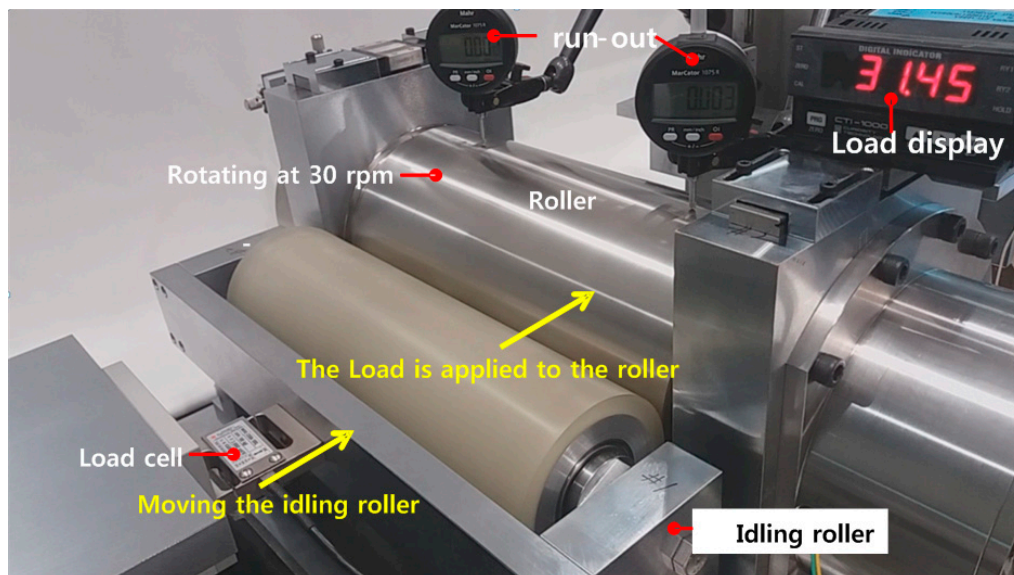


Figure 7. Vibration measurement test of precision roller for printing with magnetic bearings depending on load. Supplementary material, Video S1 is provided for this test.

4.1. Vibration Performance of Roller under Radial Loads

A load was applied through the idle roller onto the printing roller and its value was measured using a load cell attached to the fixture of the idle roller. Figure 8 shows the results of measuring the vibration amount of the roller depending on the load condition of the roller using the gap sensors of the left and right radial magnetic bearings. The vibration was first measured without contact with the idle roller under stop condition and at 30 rev/min (Figure 8a,b). The maximum vibration measured under the stop condition was approximately 2.2 μm (peak-to-peak) while the maximum vibration at 30 rev/min was approximately 3.6 μm (peak-to-peak). Next, the roller was tested at 30 rev/min under a 300 N lateral load from the idle roller which rotates at 51 rev/min or 0.85 Hz (Figure 8c). The maximum vibration measured in the 30 rev/min rotation and 300-N maximum load condition was approximately 4.6 μm (peak-to-peak). In this case, the vibration component of the rotation frequency of the idle roller (0.85 Hz) was found to be the largest source of vibration. These vibrations are originated from all components of the system including the vibration caused by the magnetic levitation of the roller, the roundness error of the shaft core, vibration of the driving motor or from the idle roller, the mass unbalance of the roller and from sensor noise.

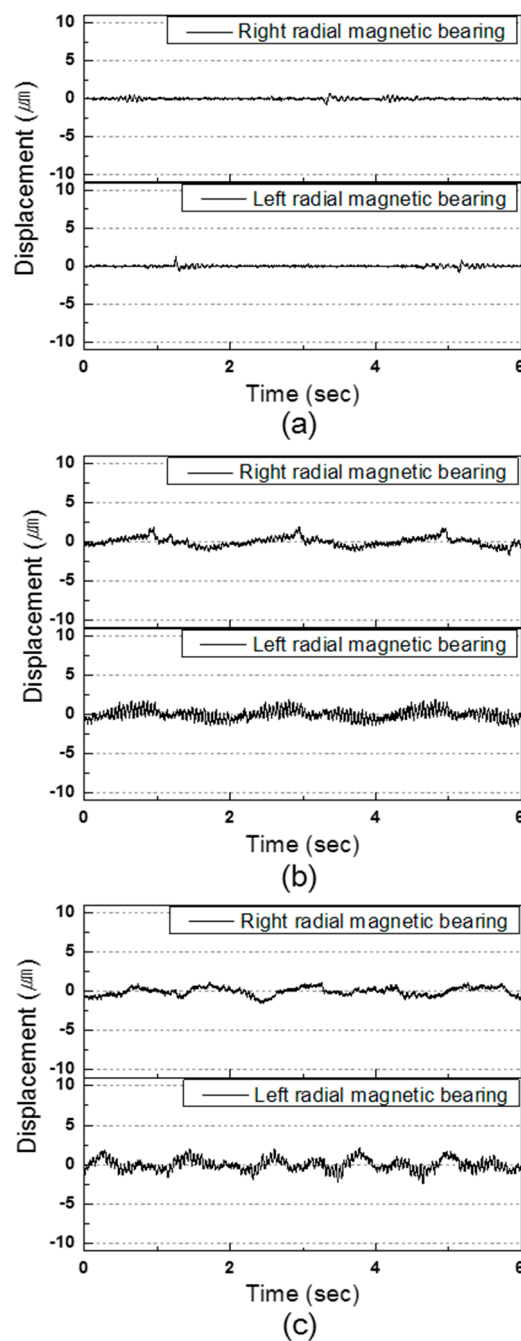


Figure 8. Vibration due to the load during the magnetic levitation of the roller: (a) stop condition (0 rev/min, 0 N); (b) rotation condition (30 rev/min, 0 N); and (c) rotation condition under a force load (30 rev/min, 300 N).

During rotation, a larger harmonic vibration was measured at the left bearing than at the right bearing. This appears to be because of the impact of the torque ripple in the motor located on the left end. The frequency of this vibration was 78 Hz, which is the 156th harmonic component corresponding to the least common multiple of 12-pole and 39-slot. It was confirmed that the roller with magnetic bearings was capable of a rotational vibration performance of less than $4.6 \mu\text{m}$ (peak-to-peak) even when applying a large lateral force of 300 N at a rotational speed of 30 rev/min.

4.2. Step Movement Control Performance of Roller

Another function that the roller must meet is the ability to accurately execute step movement position control to be able to calibrate the roller without disassembly of the entire system. The next section shows the performance of the roller to execute step movements of different heights in order to evaluate in advance how small the resolution of the step movement that the roller is able to perform.

The magnetic bearings perform feedback control to constantly position the shaft core at the reference position, which is the center of the magnetic bearing stator core, by measuring the error between the actual position of the shaft core and the reference position and compensating for the error. The reference positions of the left and right radial magnetic bearings are moved in the radial direction to perform a step movement. The resolution and settling time for step movements of 10 and 1 μm was measured with step movements being executed at constant intervals of 2 s. After five steps, the reference positions were moved back to the origin in five steps.

In the 10 μm movement test, an overshoot of approximately 20% occurred after the movement with a rising time of 0.047 s, and the movement to the reference position was performed with a 3% settling time of 0.47 s (Figure 9a). Position control with a resolution of approximately 1 μm was also confirmed to be possible using magnetic bearings, which would be useful for the superimposed printing of precise patterns (Figure 9b).

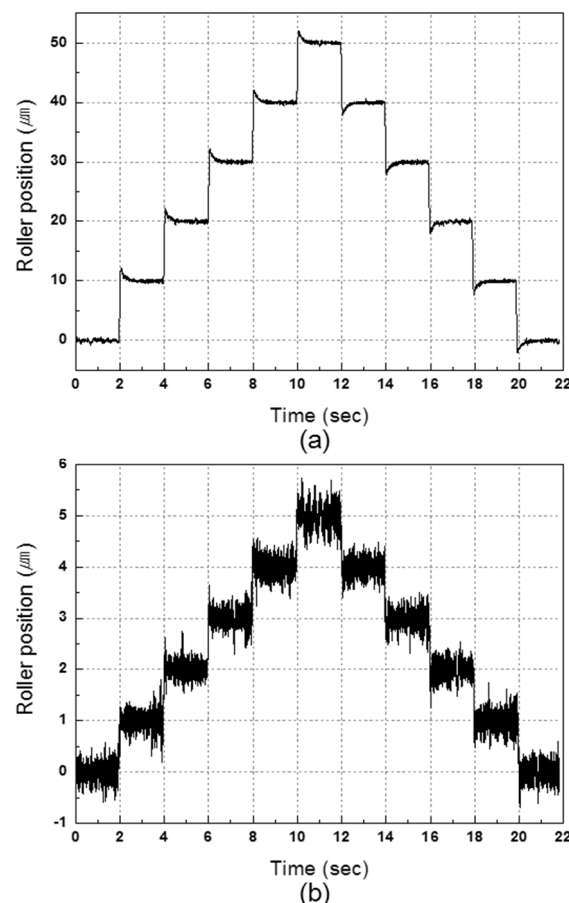


Figure 9. Step movement test results of the roller with magnetic bearings: (a) 10 μm movement; and (b) 1 μm movement.

5. Automatic Alignment Function Test of Precision Roller with Magnetic Bearings

The ability to perform automatic alignment is one of the main advantages of using magnetic bearings for precision rollers. This can be done without disassembly and can be easily adjusted and

calibrated between production batches. This section introduces two methods for automatic alignment of the roller.

5.1. Automatic Alignment Test of Roller

The basic automatic alignment method of the roller is shown in Table 2 and Figure 10. Figure 11 shows the simple schematic of the automatic alignment function test device using load cells. When the roller contacts the alignment reference surface, the contact forces at both ends of the roller are measured and these contact forces are compared to align the roller. Load cells, which can simultaneously measure the force applied at each end and play the role of the alignment reference, were installed at the left and right ends of the roller. Although both load cells have different distances from the origin of the roller, they are located within closer distances than the magnetic bearing air gap (0.2 mm), in which the roller can move. Figure 12 shows the experimental setup for the automatic alignment test. After levitating the roller to the origin with magnetic bearings, misalignment is forcibly formed by placing both load cells at different distances from the roller surface within the range of the air gap (± 0.2 mm) of the radial magnetic bearings. The reference force used to determine whether the roller contacted the load cells (alignment reference surface) was set to 5 N, and the forces applied to the load cells were measured while the roller was moved toward the load cells with a constant fine displacement (here 5 μ m). The fine displacement movement of the magnetic bearings was stopped when contact forces exceeding 5 N were measured by both load cells.

Table 2. Sequence of steps for automatic alignment of roller.

Step	
1	A load cell for measuring the contact forces between the roller and counterpart surface is installed at each end of the roller. Here, each load cell is installed to create misalignment within the air gap (± 0.2 mm) of the roller surface and radial magnetic bearings.
2	The reference force used to determine whether the roller contacted the counterpart surface is set.
3	The reference position of the roller shaft in the radial magnetic bearings is modified so that the roller can move toward the counterpart surface (load cell) at a constant displacement. Through this, the roller moves by a fine displacement.
4	When the roller contacts a load cell, the load cell can measure the contact force. The fine displacement movement is repeated until the contact force is measured.
5	The contact forces measured through the load cells at the magnetic bearings of both ends are compared with the reference force. If the contact forces are smaller than the reference force, the fine displacement movement is repeated. Otherwise, contact is determined and the movement is stopped.

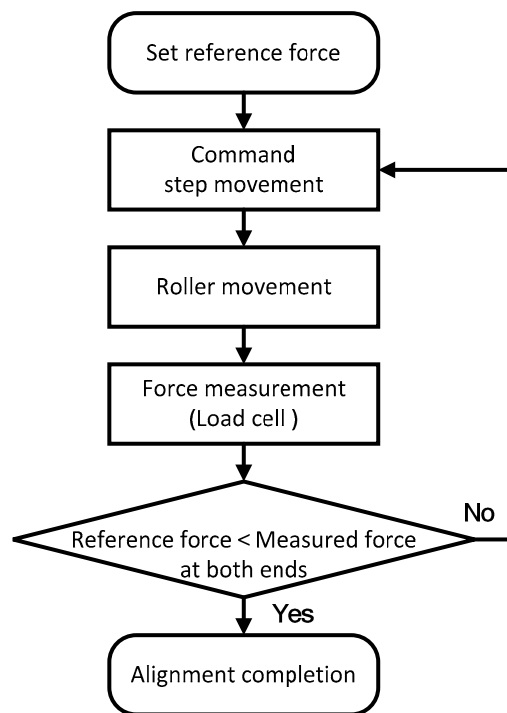


Figure 10. Flow chart for automatic alignment.

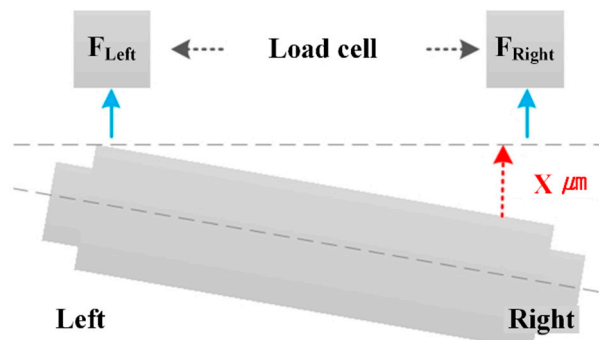


Figure 11. Schematic of automatic alignment test for roller with magnetic bearings.

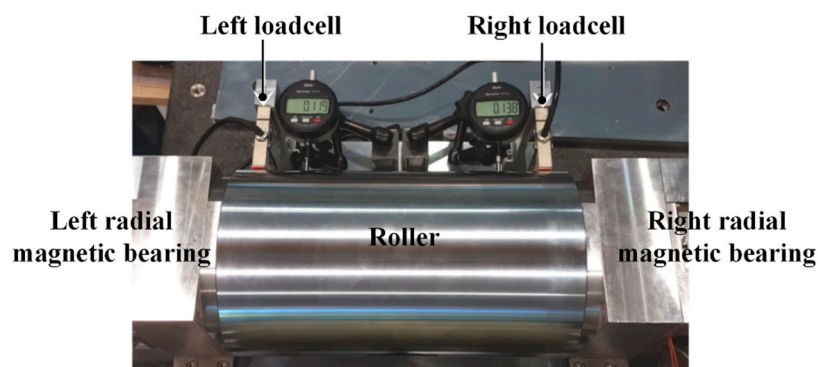


Figure 12. Experimental setup for automatic alignment test for the roller with magnetic bearings using load cells.

Figure 13 shows the results of testing the automatic alignment function of the roller moved by $5 \mu m$. ① The right load cell started to detect force from $20 \mu m$ based on the origin, and ② stopped moving at $60 \mu m$. ③ The left load cell started to detect force from $65 \mu m$, and ④ stopped moving at

120 μm , completing automatic alignment. Through this, it could be predicted that the left-end and right-end misalignments of the roller for the load cells (counterpart surface) were approximately 60 μm . The time spent for the automatic alignment was approximately 17 s. After alignment, the measured contact force was 7.4 N for the right end and 5.2 N for the left end. An approximate difference of 2.2 N was measured between both ends, which is 2.4 N over the reference value. Figure 14 shows the test results after setting the displacement at 10 μm to reduce the time spent for alignment.

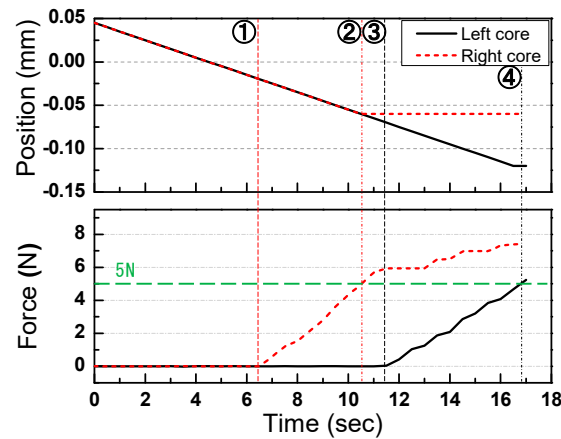


Figure 13. Test results under the reference force of 5 N and movement of 5 μm .

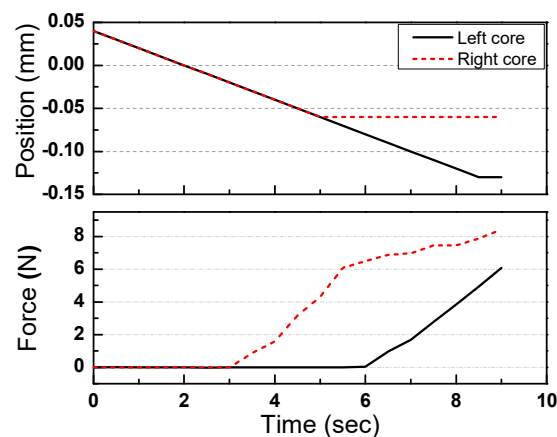


Figure 14. Test results under the reference force of 5 N and movement of 10 μm .

Although the time spent for the automatic alignment decreased to 9 s, the measured contact force was 8.3 N for the right end and 6 N for the left end after the alignments. Under both conditions, a difference in the contact force between both ends occurred after the completion of the alignment, and the end that first reached the reference force showed a larger error than the other. This appears to be because a phenomenon similar to the principle of the lever occurring due to the force sensors being not located on the inside magnetic bearings. This makes the entire roller rotate around the non-moving bearing as a pivot, which increases the force throughout. Consequently, it was confirmed that the current alignment algorithm requires improvement.

5.2. Improved Automatic Alignment Test of Roller

The error in the previous method is due to the difference between the position of the magnetic bearing shaft core, which performs position control, and the location of the magnetic bearings which perform movements of the smaller. From an alignment perspective, reducing the difference in the contact force between the left and right ends of the roller is more important than the reducing the error between the contact forces and the reference force. To reduce this difference, the automatic alignment

procedure was modified, as shown in Figure 15. First, both bearings move at a given speed (coarse step). When either end of the roller reaches the reference force first, the roller end that reached the reference force moves in the opposite direction of the printing surface at a reduced speed (fine step) to compensate for the lever effect and prevent further increase of the contact force. Movement of the roller stops when the contact forces at both ends of the roller are higher than the reference force. An estimate for the ratio of coarse step to fine step can be obtained using the principle of lever using the distance between the bearings and the distance from the bearing to the load cell. Through this method, the time spent for the contact force to reach the reference force can be reduced, the error with the reference force can be reduced, and the difference in the contact force between the left and right ends can be reduced.

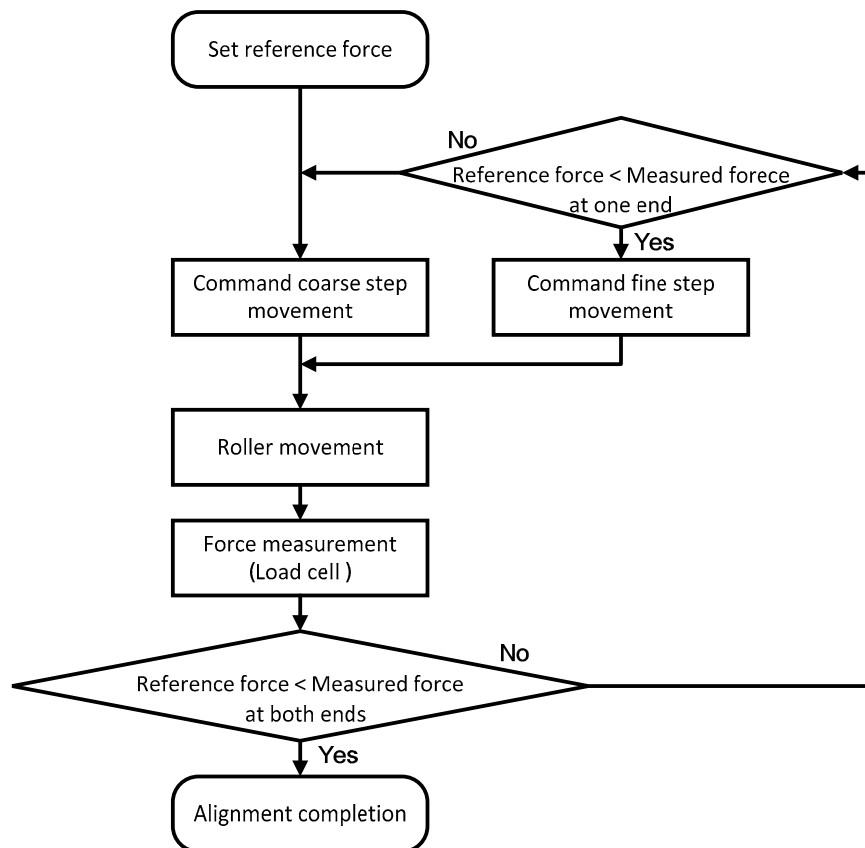


Figure 15. Flow chart for improved automatic alignment.

Figure 16 shows the results of the automatic alignment test conducted based on the improved automatic alignment procedure for a reference force of 5 N. Here, step movement of coarse mode and fine mode was selected as 10 μm and 2 μm , respectively. In the previous section, the roller was evaluated to be capable of step movement of 1- μm resolution, thus it can perform fine mode of 2- μm step movement. ① The right load cell started to detect force from 22 μm based on the origin, and ② started moving in the opposite direction in steps of 2 μm . ③ The left load cell started to detect force from 60 μm , and ④ alignment was completed once the left core moved by 130 μm . This kept the contact force of the right-end load cell nearly constant throughout the movement of the other bearing. After approximately 9 s, the alignment was completed as the measured forces on both ends of the roller exceeded the reference force. After alignment completion, the measured forces on both ends of the roller were 5.96 N and 6.12 N. The difference was 0.16 N, indicating significantly improved alignment compared to the previous automatic alignment method. Table 3 shows the results of five automatic alignment tests for the reference forces of 5 N and 10 N under random misalignment conditions. In all cases, the difference in the measured force between each end of the roller after alignment was less than 0.3 N, confirming the reliable automatic alignment function of the improved algorithm.

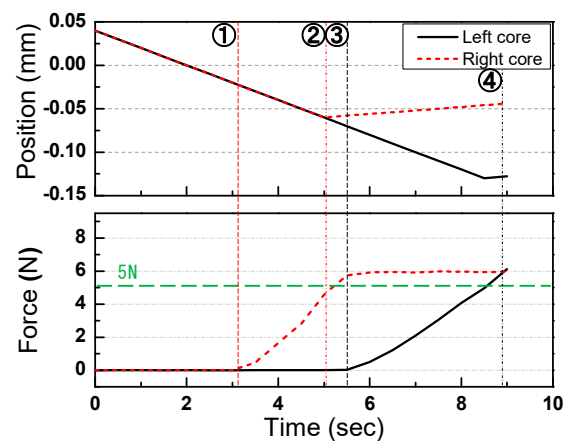


Figure 16. Test results of the improved automatic alignment control; reference force, 5 N; movement 1, 10 μm ; movement 2, 2 μm .

Table 3. Automatic alignment test results for random misalignment.

Test No.	Reference Force	Measured Force Error between Both Ends of the Roller
1	5 [N]	0.15 [N]
2	5 [N]	0.24 [N]
3	5 [N]	0.12 [N]
4	10 [N]	0.21 [N]
5	10 [N]	0.16 [N]

5.3. Prescale Film Test

The effectiveness of the automatic alignment of the roller was tested using a prescale film (LLW, Fujifilm Co., Tokyo, Japan), which can visually confirm the force distribution of the roller (Figure 17a). The prescale film is a kind of pressure-sensitive film that changes color depending on the pressing force [13]. This sort of automatic alignment could be practically realized by attaching load beneath the base plate of the printing equipment shown in Figure 17a. The prescale film tests were performed under two conditions, in which the base plate and roller were misaligned and aligned, respectively, and the results were compared. First, a force of 250 N was applied to the prescale film with a roller under the misalignment condition, and the result is shown in Figure 17b. Then, the roller was aligned with the base plate using the automatic alignment procedure and forces of 250 and 500 N were applied onto the prescale film by the roller. These results are shown in Figure 17c,d. The effectiveness of the automatic alignment of the roller can be visually confirmed through the uniform width of the marks on the prescale film.

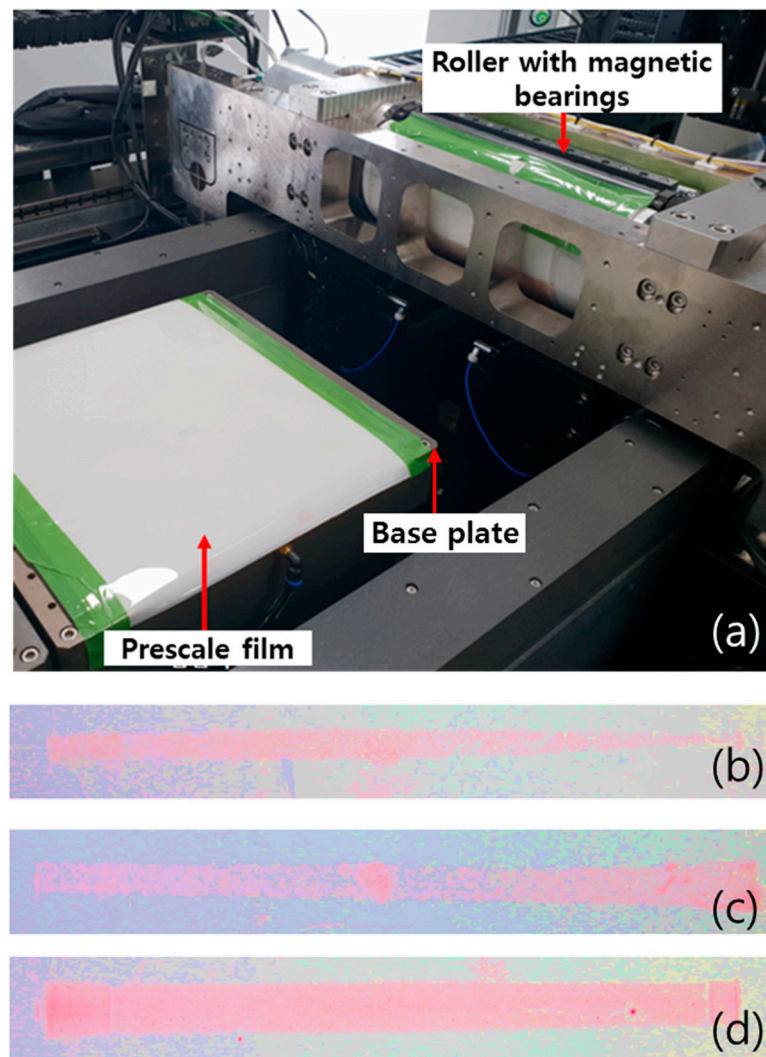


Figure 17. (a) Experimental setup and test results of force distribution (b) before and (c), (d) after roller alignment.

6. Conclusions

In this study, the automatic alignment of the precision roller for printing was implemented using the ability of magnetic bearings to move the position of the roller within the air-gap range. A precision roller for printing capable of ± 0.2 mm movement and magnetic bearings were designed and fabricated. When the precision roller contacted the alignment reference surface, the contact forces at both ends of the roller could be measured using load cells. An automatic alignment produce was developed by using the forces measured by the load cells as feedback. The improved alignment was implemented by applying two-step displacements, and the difference in the contact forces between each end was within 0.3 N. Vibrations of less than approximately 2 μm peak-to-peak was confirmed under the no-load condition and of less than approximately 5 μm peak-to-peak was observed under a rotation speed of 30 rev/min and a load of 300 N. This vibration is very small compared to the vibration of 10–100 μm peak-to-peak of conventional printing rollers supported by ball bearings [13].

The proposed system is the first magnetic bearing system designed to produce a controllable lateral load onto an external object, making it superior in terms of energy, time and quality to existing systems. If the proposed magnetic bearing roller system is used, it is expected that the disassembly–assembly process for the realignment of the assembled roller will not be necessary. In addition, the proposed system will also provide significant benefits in terms of the cost and volume because additional

actuators required for uniform printing force control on both ends of the roller will not be necessary. The lower friction of the bearings will also make the system more energy efficient and prevent printing failures, which makes the system greener. In the future, the vibration performance of the roller will be further improved by applying additional control algorithms against loads and disturbances that may occur in printing equipment, such as printed electronics equipment. In addition, improved control algorithms will be used to automate the fine adjustments near the setpoint.

Supplementary Materials: The following are available online at <http://www.mdpi.com/2076-3417/9/20/4389/s1>, Video S1: Vibration Performance of Roller under Radial Loads.wmv.

Author Contributions: Conceptualization, C.H.P.; methodology, D.K.; software, C.H.P. and T.G.Y.; validation, D.K.; writing—original draft preparation, C.H.P., T.G.Y., and H.R.; writing—review and editing, C.H.P. and H.R.; supervision, C.H.P.; and funding acquisition, C.H.P.

Funding: This research was funded by the R&D Program (No. R0005638) of the Ministry of Trade, Industry & Energy (MOTIE), Korea Institute for Advancement of Technology (KIAT) through the Encouragement Program for The Industries of Economic Cooperation Region.

Conflicts of Interest: The authors declare no conflict of interest.

References

1. Søndergaard, R.R.; Hösel, M.; Krebs, F.C. Roll-to-Roll fabrication of large area functional organic materials. *J. Polym. Sci. Pol. Phys.* **2013**, *51*, 16–34. [CrossRef]
2. Noh, J.H.; Kim, I.; Park, S.H.; Jo, J.; Kim, D.S.; Lee, T.-M. A study on the enhancement of printing location accuracy in a roll-to-roll gravure offset printing system. *Int. J. Adv. Manuf. Technol.* **2013**, *68*, 1147–1153. [CrossRef]
3. Choi, Y.M.; Lee, E.; Lee, T.M. Mechanism of reverse-offset printing. *J. Micromech. Microeng.* **2015**, *25*, 1–7. [CrossRef]
4. Choi, Y.M.; Lee, E.S.; Lee, T.M.; Kim, K.Y. Optimization of a reverse-offset printing process and its application to a metal mesh touch screen sensor. *Microelectron. Eng.* **2015**, *134*, 1–6. [CrossRef]
5. Sievers, L.; Ballas, M.J.; Flotow, A.V. Modeling of Web Conveyance Systems for Multivariable Control. *IEEE Trans. Automat. Contr.* **1988**, *33*, 524–531. [CrossRef]
6. Brandenburg, G. New Mathematical Models and Control Strategies for Rotary Printing Presses and Related Web Handling Systems. *IFAC Proc. Vol.* **2011**, *44*, 8620–8632. [CrossRef]
7. Brändlein, J.; Eschmann, P.; Hasbargen, L.; Weigand, K. *Ball and Roller Bearings: Theory, Design and Application*; Wiley: Hoboken, NJ, USA, 1999; ISBN 978-0-471-98452-8.
8. Raul, P.R.; Manyam, S.G.; Pagilla, P.R.; Darbha, S. Output regulation of nonlinear systems with application to roll-to-roll manufacturing systems. *IEEE/ASME Trans. Mechatron.* **2015**, *20*, 1089–1098. [CrossRef]
9. Ahn, S.H.; Guo, L.J. Large-area roll-to-roll and roll-to-plate nanoimprint lithography: A step toward high-throughput application of continuous nanoimprinting. *ACS Nano* **2009**, *3*, 2304–2310. [CrossRef] [PubMed]
10. Libert, A.M. Precision Control of Cylindrical Stamp Contact in a Continuous Roll-to-Roll Microcontact Printing Machine. Master Thesis, Massachusetts Institute of Technology, Boston, MA, USA, 20 May 2014.
11. Petrzela, J.E.; Hale, M.R.; Hardt, D.E. Contact pattern sensitivity and precision machine control in roll-to-roll microcontact printing. In Proceedings of the Materials Research Society Symposia, Boston, MA, USA, 25 November 2012.
12. Kang, D.; Lee, E.; Kim, H.; Choi, Y.M.; Lee, S.; Kim, I.; Yoon, D.; Jo, J.; Kim, B.; Lee, T.M. Investigation on synchronization of the offset printing process for fine patterning and precision overlay. *J. Appl. Phys.* **2014**, *115*, 234908. [CrossRef]
13. Choi, Y.M.; Kang, D.; Lim, S.; Lee, M.G.; Lee, S.H. High-Precision Printing Force Control System for Roll-to-Roll Manufacturing. *IEEE/ASME Trans. Mechatron.* **2017**, *22*, 2351–2358. [CrossRef]
14. Schweitzer, G.; Maslen, E.H. *Magnetic Bearings: Theory, Design and Application to Rotating Machinery*; Springer: Berlin, Germany, 2009; ISBN 978-3-642-00496-4.

15. Lum, K.Y.; Coppola, V.T.; Bernstein, D.S. Adaptive autocentering control for an active magnetic bearing supporting a rotor with unknown mass imbalance. *IEEE Trans. Control Syst. Technol.* **1996**, *4*, 587–597. [[CrossRef](#)]
16. Park, C.H.; Yoon, T.G.; Park, J.Y. Design of magnetic bearings for 200 HP class turbo blower. *KSFM* **2015**, *18*, 12–18. [[CrossRef](#)]
17. Zheng, S.; Li, H.; Han, B.; Yang, J. Power consumption reduction for magnetic bearing systems during torque output of control moment gyros. *IEEE Trans. Power Electron.* **2017**, *32*, 5752–5759. [[CrossRef](#)]
18. Jungmayr, G.; Loeffler, J.; Winter, B.; Jeske, F.; Amrhein, W. Magnetic gear: Radial force, cogging torque, skewing, and optimization. *IEEE Trans. Ind. Appl.* **2016**, *52*, 3822–3830. [[CrossRef](#)]
19. Knospe, C.R. Active magnetic bearings for machining applications. *Control. Eng.* **2007**, *15*, 307–313. [[CrossRef](#)]
20. Park, C.H.; Choi, S.K.; Ahn, J.H.; Ham, S.Y.; Kim, S.H. Thrust hybrid magnetic bearing using axially magnetized ring magnet. *J. Magn.* **2013**, *18*, 302–307. [[CrossRef](#)]
21. Park, C.H.; Choi, S.K.; Ham, S.Y. Design of magnetic bearing for turbo refrigerant compressors. *Mech. Ind.* **2014**, *15*, 245–252. [[CrossRef](#)]



© 2019 by the authors. Licensee MDPI, Basel, Switzerland. This article is an open access article distributed under the terms and conditions of the Creative Commons Attribution (CC BY) license (<http://creativecommons.org/licenses/by/4.0/>).